Hindawi Publishing Corporation
Journal of Chemistry
Volume 2016, Article ID 7936258, 8 pages
http://dx.doi.org/10.1155/2016/7936258

Research Article

A Comparison Study of Mechanism: Cu^{2+} Adsorption on Different Adsorbents and Their Surface-Modified Adsorbents

Yaqin Yu, Xinrui Li, and Jiemin Cheng

College of Geography and Environment, Shandong Normal University, Jinan 250014, China

Correspondence should be addressed to Jiemin Cheng; jmcheng2002@hotmail.com

Received 11 October 2015; Accepted 15 December 2015

Academic Editor: Suvardhan Kanchi

The isothermal adsorption kinetics of Cu^{2+} onto Carbon Black (CB) and Oxidized Carbon Black (OCB) were studied under different solution conditions and compared with bentonite and organic bentonite with the hexadecyltrimethylammonium bromide (HDTMA). The adsorption capacities followed the order of OCB > CB > organic bentonite > bentonite, which was consistent with the orders of their surface roughness and specific surface area. The Fourier transmission infrared (FT-IR) spectroscopy, scanning electron microscopy (SEM), and transmission electron microscope (TEM) were used to explore the adsorption mechanism at molecular level. The adsorption process onto CB was physical adsorption. However, with the increase of oxygen-containing functional groups (C=O, C-O, and CNO), the chelation adsorption onto OCB became gradually dominant except physical adsorption. The ion exchange adsorption was the major adsorption mechanism of bentonite. The compounds were introduced into clay interlayer by complexing reaction with Cu^{2+}, which improved the adsorption capacity of organic bentonite. The results present a significant implication for the environmental fate assessment of heavy metal pollution.

1. Introduction

In recent decades, increased copper (Cu) contamination in soil has created a global concern [1]. It is known that prolonged exposure to Cu compounds can have negative impacts on organism, plants, and human health through the circulation of food chain [2–5]. The heavy metal contaminants are difficult to remove by biodegradation. Therefore, the protection and restoration of Cu^{2+} contaminated soils generate a great demand of developing novel remediation technologies.

Chinese soil contaminants were difficult to remove because of their low concentration and complicated composition [6]. Compared with other techniques, adsorption is one of the best available treatment technologies for Cu^{2+} removal from soil, because it is simple, safe, easy to operate, and highly efficient. The most important criterion for adsorption technique is the selectivity of efficient adsorbents with high adsorption capacity and cost efficiency. The common adsorbents, such as activated carbon [7], dolomite [8], chitosan [9], and pomegranate peel [10], have been developed and expressed high-effective adsorption of heavy metal. However, there are quite few studies on their adsorption mechanism.

The nanometer materials have the unique properties of huge specific surface and high-effective activity. Carbon Black (CB) is a typical nanomaterial, formed form the incomplete combustion of organism and fossil fuels [11, 12]. According to extensive studies, CB is a hydrophobic and nonpolar adsorbent and has strong adsorption ability for organic contaminants (including pesticides, phenanthrene, and cyclic amines) [13–16]. Concurrently, surface-modified CB has high adsorption capacity of heavy metals [17, 18]. However, its adsorption mechanism remains little known.

Bentonite consists of two silica sheets' sandwich and one water-aluminum layer. Recent studies have regarded it as a natural adsorbent with high adsorption capacity and ion exchange property [19]. Although the modified bentonite has high adsorption capacities of organics (including propylmercaptan, aroma compounds, and dye) [20, 21], it is less efficient for heavy metals. In addition, its reaction mechanism is not still adequately known. So the further exploration of its reaction mechanism is crucial for improvement of adsorption efficiency.

In this study, we evaluated the adsorption potential of four adsorbents (CB, OCB, bentonite, and organic bentonite)

Table 1: The properties of Carbon Black.

Property	Value	Test method
Heating loss/%	1	ISO 1126 [27]
Iodine number/($g \cdot kg^{-1}$)	700–900	ISO 1304 [28]
Ash content/%	5–8	ISO 1125 [29]
Density/($kg \cdot m^{-3}$)	340	ISO 1306 [30]
pH value	9.1	ASTM D 1512 [31]

for Cu^{2+} and further investigated the adsorption mechanisms of Cu^{2+} to different adsorbents on molecular scale. Batch adsorption experiments and related characterization techniques including Fourier transmission infrared (FT-IR) spectroscopy, scanning electron microscopy (SEM), and transmission electron microscope (TEM) were used to explore the adsorption mechanism. The results present an innovative material for developing remedy technology of heavy metal pollution.

2. Materials and Methods

2.1. Chemicals and Materials. Carbon Black (CB) was purchased from Jinan Tiancheng factory, mean particle size 30–60 nm. Table 1 briefly overviews some properties of black carbon.

Bentonite was purchased from Shanghai Crystal Pure Biological Technology Co., Ltd., cation exchange capacity of 945 $mmol \cdot kg^{-1}$ and montmorillonite content of 85%. Chemicals used in the study are all analytic pure. Concentrated Nitrate Acid (65%) and Potassium Permanganate ($KMnO_4$) were purchased from Tianjin Hongyan Chemical Reagent Factory; HDTMA was supplied from Tianjin Guangfu Chemical Research Institute; copper sulfate pentahydrate ($CuSO_4 \cdot 5H_2O$) was obtained from Sinopharm Chemical Reagent Co., Ltd.

2.2. Preparation of Modified Adsorbents. Oxidized Carbon Black (OCB) was performed by oxidizing CB with concentrated nitrate acid and potassium permanganate. Briefly, 10 g CB was mixed with 110 mL acidic potassium permanganate solution in 250 mL conical beakers under the condition of water bath at 90°C for 3.0 h. Subsequently, the products were separated and washed with deionized water until the pH of filtrate remained at 5.5. After it dried in oven at 80°C for 7.0 h, the OCB were obtained.

Organic Bentonite was prepared by suspension wet process, with 10% concentration of suspension and the following condition, $W_{HDTMA} : W_{Bentonite} = 1 : 2$ (quality ration) and pH = 7. They were mixed in bath oscillator (90°C) for 2.5 h, and then the products were filtered. The solid was washed with deionized water to remove HDTMA and further dried at room temperature.

2.3. Batch Adsorption Experiments

2.3.1. Adsorption Kinetics. Batch adsorption experiments of absorbing Cu^{2+} on the different adsorbents were conducted to compare the adsorption rate. The adsorption kinetics study of CB (OCB) was performed by adding 0.1 g sample and 20 mL 180 $mg \cdot L^{-1}$ Cu^{2+} solution in 100 mL vials. Then all vials were shaken at 25°C for 240 min. The adsorption kinetics study of bentonite (organic bentonite) was performed by mixing 0.2 g samples with 20 mL 80 $mg \cdot L^{-1}$ Cu^{2+} solution and was shaken at 25°C for 240 min.

2.3.2. Adsorption Isotherms. First, 0.1 g CB (OCB) was mixed with 20 mL varying initial concentrations (20–180 $mg \cdot L^{-1}$) Cu^{2+} solution in 100 mL vials and shaken for 3.0 h. In addition, adsorption of bentonite (organic bentonite) was investigated by adding 0.2 g samples to 20 mL Cu^{2+} solution with varying initial concentrations (10–120 $mg \cdot L^{-1}$) at the desired pH. Then the mixtures were shaken for 2.0 h and future kept in incubator for 24 h at 25°C. Finally, the Cu^{2+} concentration was determined using an 800 atomic adsorption spectroscopy.

2.4. Characterization. The functional groups on the adsorbents were analyzed using Fourier transmission infrared spectroscopy (Fourier-380 FTIR, USA). The FTIR spectra were recorded in the 400–4000 cm^{-1} spectral range by using KBr pellet method with a Fourier-380 FTIR spectrometer at a standard resolution of $\pm 2\ cm^{-1}$. The surface morphology of the adsorbents was examined using a scanning electron microscopy (H-800 EM, Japan). The internal structure of CB, OCB, bentonite, and organic bentonite was examined using transmission electron microscope (H-800 EM, Japan).

2.5. Analysis of Data. All adsorption data were obtained in duplicate experiments. Two different isotherm models were employed to fit the adsorption equilibrium isotherm:

Langmuir model:

$$q_e = \frac{K_L q_{max} C_e}{1 + K_L C_e}. \quad (1)$$

Freundlich model:

$$q_e = K_f C_e^{1/n}, \quad (2)$$

where q_e ($mg \cdot g^{-1}$) is the adsorption amount of Cu^{2+}; C_e ($mg \cdot L^{-1}$) is the adsorption equilibrium concentration of Cu^{2+}; q_{max} ($mg \cdot g^{-1}$) is the maximum adsorption capacity; K_L ($L \cdot mg^{-1}$) is the Langmuir adsorption affinity constant; K_f and n are the Freundlich adsorption constants representing the adsorption capacity and the adsorption intensity, respectively.

3. Results and Discussion

3.1. Adsorption Kinetic Studies. The adsorption kinetic curves of Cu^{2+} on CB, OCB, bentonite, and organic bentonite at 25°C show similar features (Figure 1). The adsorption process

Table 2: Parameters of adsorption kinetics model of Cu(II) on CB and bentonite.

Number	Treatment	Pseudo first-order model			Pseudo second-order model		
		q_{1e} (mg/g)	k_1 (1/min)	R^2	q_{2e} (mg/g)	k_2 (g/mgL·min)	R^2
a	CB	12.265	0.061	0.989	12.628	0.016	0.982
b	OCB	20.053	0.055	0.940	20.877	0.007	0.998
c	Bentonite	10.473	0.097	0.893	10.534	0.113	0.999
d	Organic bentonite	11.185	0.112	0.872	11.213	0.244	0.999

Table 3: Parameters for adsorption isotherm of Cu(II) on CB and bentonite.

Number	Treatment	Langmuir			Freundlich		
		$q_{\max}$ (mg/g)	K_L (L/mg)	R^2	K_F (mg/g) (L/mg)$^{1/n}$	$1/n$	R^2
a	CB	16.507	0.021	0.995	1.229	0.507	0.995
b	OCB	23.419	0.091	0.963	4.427	0.379	0.992
c	Bentonite	7.059	0.578	0.972	3.686	0.468	0.924
d	Organic bentonite	11.168	0.098	0.976	1.209	0.645	0.799

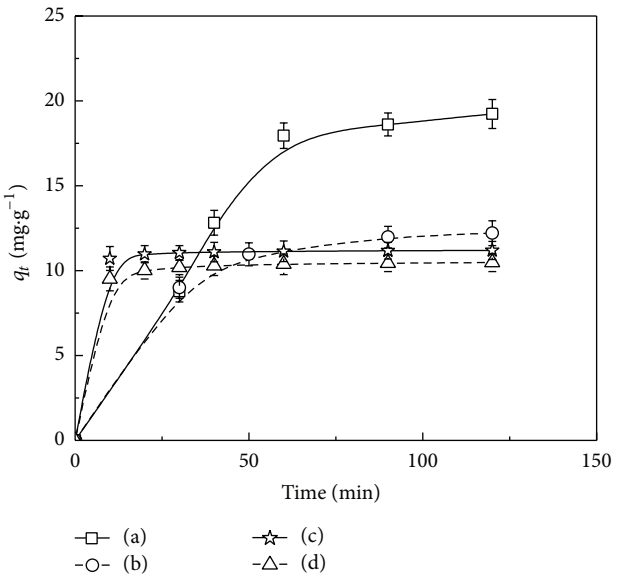

Figure 1: Adsorption kinetics for Cu^{2+} adsorption on (a) OCB, (b) CB, (c) organic bentonite, and (d) bentonite as a function of reaction time.

of four materials is at the fast reaction stage at first, and slowed down with time. The adsorption kinetics of Cu^{2+} by CB and OCB are rapid for the first 40 min and then gradually reach equilibrium in about 70 min. Similarly, the adsorption kinetics of Cu^{2+} by bentonite and organic bentonite are rapid for the first 10 min and then gradually reach equilibrium in about 20 min. As shown, the adsorption capacities follow the order of OCB > CB > organic bentonite > bentonite.

Figure 2 shows the data fitted with the mass transfer model. The R^2 values obtained using the pseudo first-order model and the pseudo second-order model are bigger than the first-order model and the second-order model. Compared with other models, the pseudo first-order model and the pseudo second-order model are better-fit. Table 2 indicates that the adsorption kinetics for Cu^{2+} on all materials follow the pseudo second-order model with higher R^2 (0.982–0.999), but the maximum uptake values differ. Thus, the conclusion further confirmed the phenomenon in Figure 1. Currently, it had been demonstrated that the pseudo second-order model was applied to describe chemisorption [22], but it was limited by adsorbent surface properties, adsorbate ions, and pH. The k_2 values follow the order of organic bentonite > bentonite > CB > OCB, which present the adsorption rate.

3.2. Adsorption Isotherms Studies. The adsorption of Cu^{2+} by the four adsorbents was studied in the batch mode at 25°C. The adsorption isotherms for the four adsorbents were nonlinear, and the maximum uptake values differ (Figure 3). The adsorption amounts of Cu^{2+} of the four materials increase rapidly in the low concentration range and then increase gradually as the initial concentrations increase.

The equilibrium adsorption isotherm data and related isotherm parameters were analyzed using both Langmuir and Freundlich isotherm (Table 3). The correlation coefficient (R^2) values demonstrate that the Langmuir model is more suitable than the Freundlich model, except for OCB. These results indicate that the adsorption mechanisms of Cu^{2+} on these adsorbents are different. The adsorption process of CB, bentonite, and organic bentonite is surface adsorption. Ion exchange adsorption is the main adsorption mechanism of bentonite and organic bentonite, which have exchangeable cations. However, the adsorption mechanism of OCB is chelation in addition to surface adsorption. The maximum adsorption capacity follows the order of OCB > CB > organic bentonite > bentonite, consistent with surface area and oxygen-containing functional groups.

3.3. Properties of Different Adsorbents. The physicochemical properties of different adsorbents are shown in Table 4.

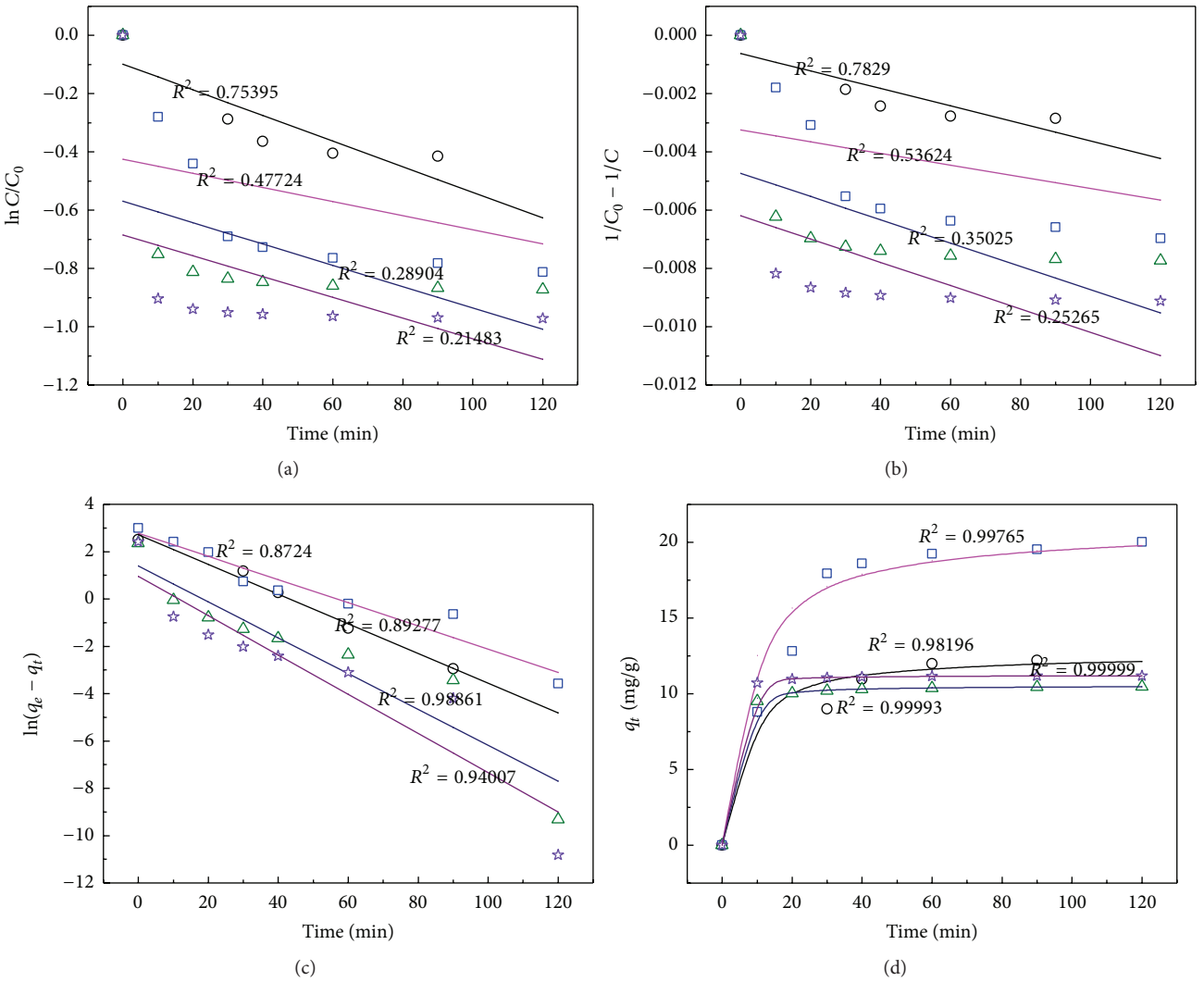

Figure 2: Four kinetic models for the adsorption of Cu^{2+} by OCB, CB, organic bentonite, and bentonite. The solid line is the fit to the four order models: (a) the first-order model, (b) the second-order model, (c) the pseudo first-order model, and (d) the pseudo second-order model.

Table 4: Characteristics of different adsorbents.

Number	Treatment	pH	Surface area ($m^2 \cdot g^{-1}$)	Zeta potential
a	CB	9.1	931.33	−6.06
b	OCB	6.0	1114.23	−17.18
c	Bentonite	10.2	9.54	−17.50
d	Organic bentonite	8.3	10.67	−9.46

CB and bentonite are alkaline in nature, while surface modification results in the decreasing of pH. The specific surface area follows the order of OCB > CB > organic bentonite > bentonite, which further demonstrates the previous conclusion. Compared with bentonite, the negative charge amount of organic bentonite decreases, which is inconsistent with the adsorption capacity. That is because the organic compounds introduced in clay interlayer occur as complexing reaction with heavy metal ions in addition to exchange adsorption [23].

3.3.1. IR Analysis. FTIR spectra of CB, OCB, bentonite, and organic bentonite were recorded in the 400–4000 cm^{-1} spectral range by using KBr pellet method with a Fourier-380 FTIR spectrometer, and the results are shown in Figure 4. An O-H stretching band at 3450 cm^{-1} and a C=C stretching band at 1619 cm^{-1} were typical functional group of CB. Compared with CB, both bands not only were reserved but also became much more in OCB. The bands at 1721.6 and 1244.0 cm^{-1} can be assigned to the C=O and C-O stretching vibrations, respectively. The band at 447.3 cm^{-1} can be assigned to

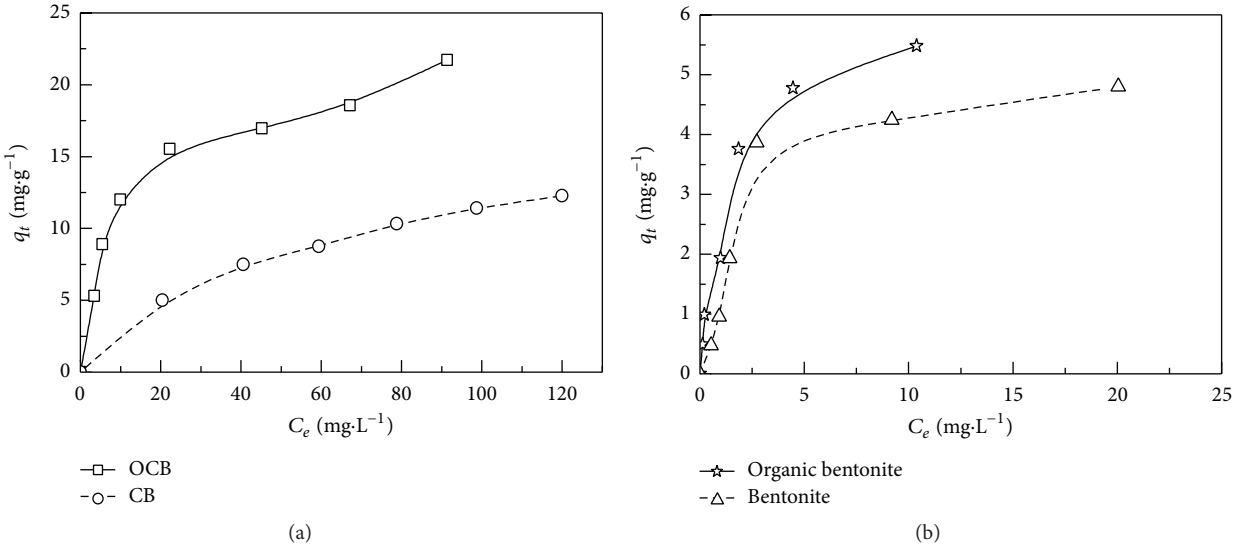

Figure 3: Sorption isotherms for the adsorption of Cu^{2+} by CB, OCB, bentonite, and organic bentonite.

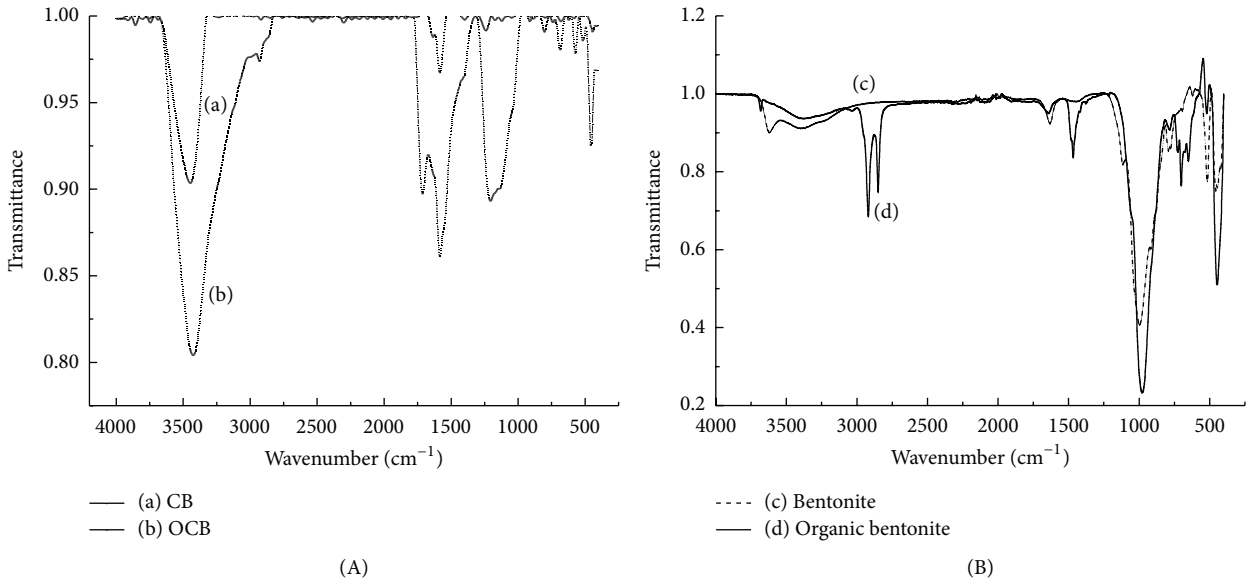

Figure 4: IR spectrum of different adsorbents. (a) CB, (b) OCB, (c) bentonite, and (d) organic bentonite.

the CNO bending vibration. All these oxygen-containing functional groups chelating with heavy metal ion were absent in CB.

The bands at 3622 and 3693 cm^{-1} can be assigned to the Al-Al-OH and Al-Mg-OH stretching vibration, respectively, which were typical groups of bentonite [24]. A broad band at 1115–996 cm^{-1} region was assigned to the Si-O stretching vibration, whereas a band at 516 cm^{-1} was assigned to the Si-O bending vibration. Compared with natural bentonite, a pair of bands at 2919 and 2849 cm^{-1} in organic bentonite was assigned to the symmetric and asymmetric C-H stretching vibrations of methyl and methylene groups. And a band at 1467 cm^{-1} was assigned to the asymmetric C-H bending vibration. These bands suggested the presence of cationic surfactants in the bentonite.

3.3.2. SEM Characterization. To investigate the surface morphology, SEM (H-800 EM, Japan) analysis was performed on the different adsorbents (Figure 5). The photographs of CB suggest sphere with diameter of 50–60 nm, which demonstrates nanoscale material. However, OCB had no obvious variation in shape and need to be further studied by TEM. In Figures 5(a) and 5(b), both materials suggest the serious aggregation of nanoparticles.

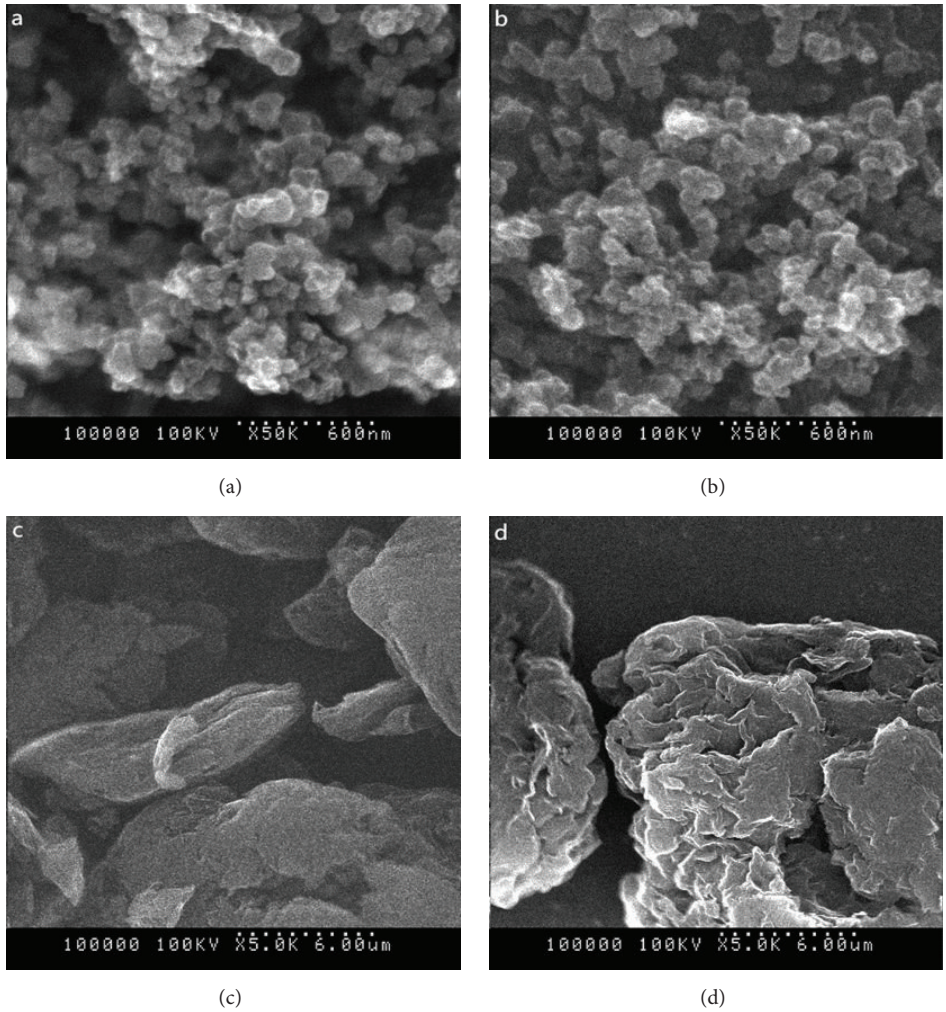

(a) (b)

(c) (d)

Figure 5: Representative SEM images of different adsorbents. (a) CB (scale bar is 600 nm), (b) OCB (scale bar is 600 nm), (c) bentonite (scale bar is 6 μm), and (d) organic bentonite (scale bar is 6 μm).

The SEM images of bentonite and organic bentonite are shown in Figures 5(c) and 5(d). The morphology of bentonite suggests smooth surface with flat crystal. Compared with natural bentonite, the clay lattice of organic bentonite appeared swollen and fluffy. This might be due to the organic compounds introduced in clay interlayer, which increase the basal spacing of clay [25]. The surface structure and porous characteristics are conductive to accelerate the spread of heavy metal ions in bentonite [26].

3.3.3. TEM Characterization. The TEM photographs of different adsorbents are shown in Figure 6. The photographs of CB suggest two components of solid and hollow sphere. Compared with CB, the OCB shows a lot of pores, which further suggests that the surface area increases. In addition, it demonstrates that CB is oxidized, which is beneficial to chelate with heavy metal ions.

As shown in Figures 6(c) and 6(d), bentonite is amorphous in structure without aggregation. The photographs of organic bentonite show some pores and blurry edges, further suggesting that the morphological structure changes by intercalation of organic compounds.

4. Conclusions

From the study, we discover that the adsorption mechanisms of Cu^{2+} on CB, bentonite, and their surface-modified materials are different. The adsorption capacities of Cu^{2+} on these adsorbents follow the order of OCB > CB > organic bentonite > bentonite, consistent with the order of their surface roughness and surface area. The results of adsorption isotherms show that the adsorption process of CB is surface adsorption, and bentonite is ion exchange adsorption because of exchangeable cations in the lattice. IR and SEM indicate that the mechanism of organic bentonite was that organic compounds introduced in clay interlayer occur as complexing reaction with heavy metal ions, in addition to exchange adsorption. However, the adsorption of OCB is that oxygen-containing functional groups chelate with heavy metal ion, by IR and TEM analysis.

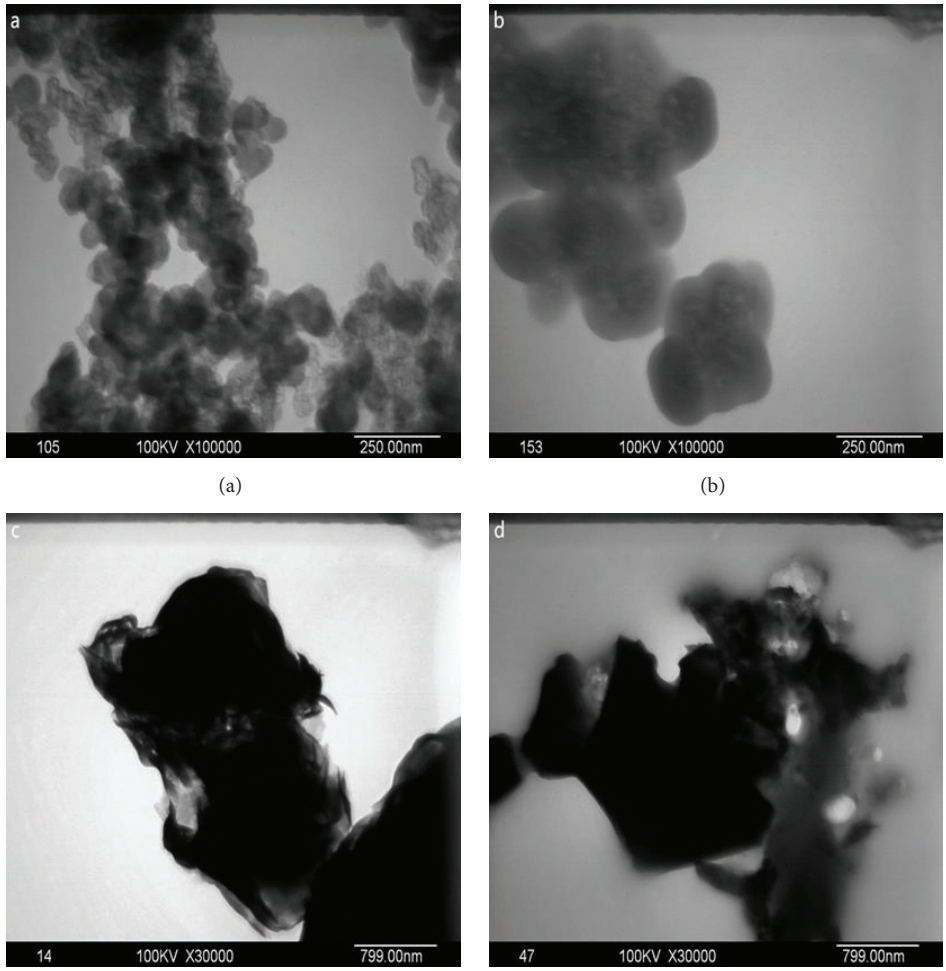

(a) (b)

(c) (d)

Figure 6: Representative TEM images of different adsorbents. (a) CB (scale bar is 250 nm), (b) OCB (scale bar is 250 nm), (c) bentonite (scale bar is 799 nm), and (d) organic bentonite (scale bar is 799 nm).

Conflict of Interests

The authors declare that there is no conflict of interests regarding the publication of this paper.

Acknowledgment

The authors would like to thank the National Natural Science Fund Committee, China (41171251) and (41471255), for financial support.

References

[1] H. Ha, J. R. Olson, L. Bian, and P. A. Rogerson, "Analysis of heavy metal sources in soil using kriging interpolation on principal components," *Environmental Science and Technology*, vol. 48, no. 9, pp. 4999–5007, 2014.

[2] A. Lerebours, G. D. Stentiford, B. P. Lyons, J. P. Bignell, S. A. P. Derocles, and J. M. Rotchell, "Genetic alterations and cancer formation in a European flatfish at sites of different contaminant burdens," *Environmental Science and Technology*, vol. 48, no. 17, pp. 10448–10455, 2014.

[3] G. K. Bielmyer-Fraser, T. A. Jarvis, H. S. Lenihan, and R. J. Miller, "Cellular partitioning of nanoparticulate versus dissolved metals in marine phytoplankton," *Environmental Science & Technology*, vol. 48, no. 22, pp. 13443–13450, 2014.

[4] J. L. Schroder, N. T. Basta, R. L. Lochmiller et al., "Soil contamination and bioaccumulation of inorganics on petrochemical sites," *Environmental Toxicology and Chemistry*, vol. 19, no. 8, pp. 2066–2072, 2000.

[5] W. S. W. Ngah and M. A. K. M. Hanafiah, "Removal of heavy metal ions from wastewater by chemically modified plant wastes as adsorbents: a review," *Bioresource Technology*, vol. 99, no. 10, pp. 3935–3948, 2008.

[6] T. Fan, W. L. Ye, H. Y. Chen et al., "Review on contamination and remediation technology of heavy metal in agricultural soil," *Ecology and Environmental Sciences*, vol. 22, pp. 1727–1736, 2013.

[7] B. M. Babić, S. K. Milonjić, M. J. Polovina, S. Čupić, and B. V. Kaludjerović, "Adsorption of zinc, cadmium and mercury ions from aqueous solutions on an activated carbon cloth," *Carbon*, vol. 40, no. 7, pp. 1109–1115, 2002.

[8] A. B. Albadarin, C. Mangwandi, A. H. Al-Muhtaseb, G. M. Walker, S. J. Allen, and M. N. M. Ahmad, "Kinetic and thermodynamics of chromium ions adsorption onto low-cost

dolomite adsorbent," *Chemical Engineering Journal*, vol. 179, pp. 193–202, 2012.

[9] D. D. Gang, B. Deng, and L. S. Lin, "As(III) removal using an iron-impregnated chitosan sorbent," *Journal of Hazardous Materials*, vol. 182, no. 1–3, pp. 156–161, 2010.

[10] E.-S. Z. El-Ashtoukhy, N. K. Amin, and O. Abdelwahab, "Removal of lead (II) and copper (II) from aqueous solution using pomegranate peel as a new adsorbent," *Desalination*, vol. 223, no. 1–3, pp. 162–173, 2008.

[11] Y. P. Qiu, H. Y. Cheng, C. Xu, and G. D. Sheng, "Surface characteristics of crop-residue-derived black carbon and lead (II) adsorption," *Water Research*, vol. 42, no. 3, pp. 567–574, 2008.

[12] J. J. Pignatello, S. Kwon, and Y. Lu, "Effect of natural organic substances on the surface and adsorptive properties of environmental black carbon (Char): attenuation of surface activity by humic and fulvic acids," *Environmental Science and Technology*, vol. 40, no. 24, pp. 7757–7763, 2006.

[13] X. S. Wang, Z. P. Lu, H. H. Miao, W. He, and H. L. Shen, "Kinetics of Pb (II) adsorption on black carbon derived from wheat residue," *Chemical Engineering Journal*, vol. 166, no. 3, pp. 986–993, 2011.

[14] Y. Yang and G. Sheng, "Enhanced pesticide sorption by soils containing particulate matter from crop residue burns," *Environmental Science and Technology*, vol. 37, no. 16, pp. 3635–3639, 2003.

[15] E. A. Yashkina, D. A. Svetlov, and S. N. Yashkin, "Adsorption of cyclic amines on graphitized thermal carbon black," *Russian Chemical Bulletin*, vol. 61, no. 8, pp. 1536–1545, 2012.

[16] G. Cornelissen and Ö. Gustafsson, "Sorption of phenanthrene to environmental black carbon in sediment with and without organic matter and native sorbates," *Environmental Science and Technology*, vol. 38, no. 1, pp. 148–155, 2004.

[17] I. Chowdhury, M. C. Duch, N. D. Mansukhani, M. C. Hersam, and D. Bouchard, "Interactions of graphene oxide nanomaterials with natural organic matter and metal oxide surfaces," *Environmental Science and Technology*, vol. 48, no. 16, pp. 9382–9390, 2014.

[18] E. Alzahrani, "Modification of activated carbon prepared from pigeon pea husks with eriochrome black T for removal of copper (II) ions," *International Journal of Recent Technology and Engineering*, vol. 3, no. 5, pp. 6–10, 2014.

[19] X.-L. Tang, X. Meng, and L. Shi, "Desulfurization of model gasoline on modified bentonite," *Industrial & Engineering Chemistry Research*, vol. 50, no. 12, pp. 7527–7533, 2011.

[20] S. Vincenzi, A. Panighel, D. Gazzola, R. Flamini, and A. Curioni, "Study of combined effect of proteins and bentonite fining on the wine aroma loss," *Journal of Agricultural and Food Chemistry*, vol. 63, no. 8, pp. 2314–2320, 2015.

[21] Q. H. Hu, S. Z. Qiao, F. Haghseresht, M. A. Wilson, and G. Q. Lu, "Adsorption study for removal of basic red dye using bentonite," *Industrial & Engineering Chemistry Research*, vol. 45, no. 2, pp. 733–738, 2006.

[22] J. Cheng, Y. Yu, T. Li, Y. Liu, and C. Lu, "A comparing study on copper adsorption on nanoscale carbon black modified by different kinds of acid," *International Journal of Nanoscience*, vol. 14, Article ID 1460024, 2015.

[23] T. S. Anirudhan, P. S. Suchithra, and P. G. Radhakrishnan, "Synthesis and characterization of humic acid immobilized-polymer/bentonite composites and their ability to adsorb basic dyes from aqueous solutions," *Applied Clay Science*, vol. 43, no. 3-4, pp. 336–342, 2009.

[24] G. Akçay and M. K. Yurdakoç, "Nonyl and dodecylamines intercalated bentonite and illite from Turkey," *Turkish Journal of Chemistry*, vol. 23, no. 1, pp. 105–113, 1999.

[25] A. Dutta and N. Singh, "Surfactant-modified bentonite clays: preparation, characterization, and atrazine removal," *Environmental Science and Pollution Research*, vol. 22, no. 5, pp. 3876–3885, 2015.

[26] C. S. Sun, Q. T. Jin, L. H. Qin, X. C. Guo, and X. Y. Liu, "The adsorption study on EDTA complexometric copper in column inorganic bentonite," *Journal of Environmental Engineering*, vol. 1, pp. 131–135, 2007.

[27] ISO, "Rubber compounding ingredients-Carbon black-Determination of loss on heating," ISO 1126-1992, 1992.

[28] ISO, "Rubber compounding ingredients—carbon black—determination of iodine adsorption number—titrimetric method," ISO 1304-1999, International Organization for Standardization, 1999.

[29] ISO, "Rubber compounding ingredients—carbon black—determination of ash," ISO 1125-1999, International Organization for Standardization, 1999.

[30] ISO, "Rubber compounding ingredients—carbon black—determination of density," ISO 1306-1995, International Organization for Standardization, 1995.

[31] ASTM, "Standard test methods for carbon black-pH value," ASTM D 1512-95, ASTM International, West Conshohocken, Pa, USA, 2000.